




# Ecological drivers of spatial community dissimilarity, species replacement and species nestedness across temperate forests

Xugao Wang<sup>1</sup>  | Thorsten Wiegand<sup>2,3</sup>  | Kristina J. Anderson-Teixeira<sup>4,5</sup> |  
Norman A. Bourg<sup>6</sup> | Zhanqing Hao<sup>1</sup> | Robert Howe<sup>7</sup> | Guangze Jin<sup>8</sup>  |  
David A. Orwig<sup>9</sup> | Marko J. Spasojevic<sup>10</sup> | Shunzhong Wang<sup>11</sup> | Amy Wolf<sup>7</sup> |  
Jonathan A. Myers<sup>12</sup>

<sup>1</sup>Key Laboratory of Forest Ecology and Management, Institute of Applied Ecology, Chinese Academy of Sciences, Shenyang, P. R. China

<sup>2</sup>Department of Ecological Modelling, Helmholtz Centre for Environmental Research-UFZ, Leipzig, Germany

<sup>3</sup>German Centre for Integrative Biodiversity Research (iDiv) Halle-Jena-Leipzig, Leipzig, Germany

<sup>4</sup>Conservation Ecology Center, Smithsonian Conservation Biology Institute, National Zoological Park, Front Royal, Virginia

<sup>5</sup>Center for Tropical Forest Science–Forest Global Earth Observatory, Smithsonian Tropical Research Institute, Panama, Republic of Panama

<sup>6</sup>U.S. Geological Survey, National Research Program – Eastern Branch, Reston, Virginia

<sup>7</sup>Department of Natural and Applied Sciences, University of Wisconsin-Green Bay, Green Bay, Wisconsin

<sup>8</sup>Center for Ecological Research, Northeast Forestry University, Harbin, China

<sup>9</sup>Harvard Forest, Harvard University, Petersham, Massachusetts

<sup>10</sup>Department of Biology, University of California Riverside, Riverside, California

<sup>11</sup>State Key Laboratory of Vegetation and Environmental Change, Institute of Botany, Chinese Academy of Sciences, Xiangshan, Beijing, China

<sup>12</sup>Department of Biology & Tyson Research Center, Washington University in St Louis, St Louis, Missouri

## Correspondence

Xugao Wang, Key Laboratory of Forest Ecology and Management, Institute of Applied Ecology, Chinese Academy of Sciences, Shenyang 110016, P. R. China.  
Email: wxg\_7980@163.com

## Abstract

**Aims:** Patterns of spatial community dissimilarity have inspired a large body of theory in ecology and biogeography. Yet key gaps remain in our understanding of the local-scale ecological processes underlying species replacement and species nestedness, the two fundamental components of spatial community dissimilarity. Here, we examined the relative influence of dispersal limitation, habitat filtering and interspecific species interactions on local-scale patterns of the replacement and nestedness components in eight stem-mapped temperate forest mega-plots at different ontogenetic stages (large versus small trees).

**Location:** Eight large (20–35 ha), fully mapped temperate forest plots in northern China and northern U.S.A.

**Time period:** 2004–2016.

**Major taxa studied:** Woody plants.

**Methods:** We combined decomposition of community dissimilarity (based on the Ružička index) and spatial point-pattern analysis to compare the spatial (i.e., distance-dependent) replacement and nestedness components of each plot with that expected under five spatially explicit null models representing different hypotheses on community-assembly mechanisms.

**Results:** Our analyses revealed complex results. In all eight forests, spatial community dissimilarity was best explained by species replacement among local tree assemblages and by a null model based on dispersal limitation. In contrast, spatial nestedness for large and small trees was best explained by random placement and habitat filtering, respectively, in addition to dispersal limitation. However, interspecific interactions did not contribute to local replacement and nestedness.

**Main conclusions:** Species replacement is the predominant process accounting for spatial community dissimilarity in these temperate forests and caused largely by local-scale species clustering associated with dispersal limitation. Nestedness, in contrast, is less prevalent and primarily associated with larger variation in local species richness as caused by spatial richness gradients or 'hotspots' of local species richness. The novel use of replacement and nestedness measures in point pattern analysis is a promising approach to assess local-scale biodiversity patterns and to explore their causes.

**Funding information**

National Natural Science Foundation of China, Grant/Award Number: 31722010 and 31770666; Chinese Academy of Sciences, Grant/Award Number: XDPB0203; National Key Research and Development Program of China, Grant/Award Number: 2016YFC0500300; Smithsonian Global Earth Observatory Initiative; HSBC Climate Partnership; International Center for Advanced Renewable Energy and Sustainability; National Science Foundation, Grant/Award Number: DEB 1557094; Tyson Research Center; The 1923 Fund; Cofrin Center for Biodiversity; European Research Council (ERC), Grant/Award Number: 233066

Editor: Andres Baselga

**KEYWORDS**

beta diversity, biotic interactions, community assembly, dispersal limitation, habitat filtering, nestedness, pattern reconstruction, point pattern analysis, species replacement

**1 | INTRODUCTION**

Disentangling the relative importance of mechanisms that create spatial variation in community composition is a central challenge in ecology and biogeography (Anderson et al., 2011; Whittaker, 1960). For example, increases in community dissimilarity (beta diversity) with spatial distance have been extensively described for diverse organisms and comprise one of the most widely recognized and important spatial biodiversity patterns (Nekola & White, 1999; Soininen, McDonald, & Hillebrand, 2007). This generalization, also called distance-decay of community similarity, is widely used in community ecology to understand processes of community assembly (Condit et al., 2002; Morlon et al., 2008; Wang et al., 2011). At biogeographical scales, patterns of spatial species turnover provide important insights into historical and regional processes underlying the composition and dynamics of regional biotas (Nekola & White, 1999; Qian & Ricklefs, 2012; Tuomisto, Ruokolainen, & Yli-Halla, 2003).

The processes that determine increasing community dissimilarity with distance (hereafter 'spatial community dissimilarity') have important implications for community assembly and the maintenance of biodiversity in ecological communities. At local scales, spatial community dissimilarity is driven by several non-mutually exclusive processes, including dispersal limitation, habitat filtering and species interactions (Morlon et al., 2008; Wang et al., 2011, 2015). Dispersal limitation (e.g., local seed dispersal) is predicted to increase spatial community dissimilarity by increasing spatial aggregation of conspecific individuals. In contrast, increased dispersal should decrease spatial community dissimilarity and homogenize community composition (Catano, Dickson, Myers, & Rejmanek, 2017; Hubbell, 2001). Likewise, habitat filtering (where species arrive at a site but fail to persist owing to the abiotic conditions; Kraft et al., 2015) can increase spatial community dissimilarities by increasing species sorting across abiotic gradients (Chase & Myers, 2011). Interspecific species interactions, such as competition or predation, can counteract positive effects of dispersal on diversity and can homogenize community composition by removing competitively inferior species or species lacking enemy-tolerant traits (Kneitel &

Miller, 2003; Mouquet & Loreau, 2003). Habitat filtering, dispersal limitation and interspecific interactions may also interact in complex ways to influence spatial community dissimilarity. For example, whereas increased dispersal may homogenize community composition under weak habitat filtering, it may increase community dissimilarity under strong habitat filtering (Myers & LaManna, 2016). Thus, patterns of spatial community dissimilarity may reflect the outcome and interplay of multiple community assembly processes.

Given the complexity of potential interactions among processes, it is not surprising that the relative importance of processes in driving patterns of spatial community dissimilarity remains largely unresolved (Svenning, Fløjgaard, & Baselga, 2011). However, these difficulties may also be grounded in an overly simplistic characterization of community dissimilarity. For example, researchers have recognized for some time that the compositional dissimilarity of two local communities may reflect two different phenomena: spatial species turnover (also known as species replacement) and nestedness (Baselga, 2010; Baselga & Leprieur, 2015; Legendre, 2014; Podani & Schmera, 2011). At one extreme (perfect species replacement), local communities contain the same number of species, but no species are shared among them. In this case, their dissimilarity is purely driven by species replacement. At the other extreme (perfect nestedness), the species composition of one local community is a completely nested subset of the other. In this case, the replacement component is zero, and the dissimilarity is entirely driven by species loss that causes nestedness. Therefore, nestedness and replacement must be disentangled at different spatial scales in order to identify the underlying, possibly antithetic, processes responsible for observed patterns of community dissimilarity (Baselga, 2010).

Species nestedness and replacement patterns have been attributed to various processes of community assembly. Previous macroecological studies showed that the nestedness component was more important in areas affected by recent glaciations (e.g., Baselga, 2010; Dobrovolski, Melo, Cassemiro, & Diniz-Filho, 2012; Svenning et al., 2011). At more local scales, nestedness patterns can emerge from habitat filtering across environmental gradients (Greve, Gremmen, Gaston, & Chown,

2005), where species that occur in harsh environments are a nested subset of species that occur in more benign environments (Chase, 2007). In contrast, species-replacement patterns at local scales are expected from neutral dynamics under dispersal limitation, ecological drift, high levels of speciation and isolation of local communities, or niche selection where different species occur under different environmental conditions (e.g., habitat filtering). Studies partitioning community dissimilarity into species replacement and nestedness components have mainly been conducted at macroecological scales (e.g., Dobrovolski et al., 2012; Svenning et al., 2011), but little is known about the relative importance of processes that influence patterns of species replacement and nestedness at local scales.

In this study, we examined the relative influence of dispersal limitation, habitat filtering and interspecific species interactions on local-scale patterns of spatial community dissimilarity and its species replacement and nestedness components in eight stem-mapped temperate forest mega-plots (20–35 ha) in the Smithsonian Forest Global Earth Observatory (ForestGEO; Anderson-Teixeira et al., 2015; Condit, 1998). Four of the temperate forest plots are located in northern China, and the other four plots in the northern U.S.A. The diversity of settings and variation in species richness among the eight forest plots (Table 1) allow us to explore the generality of the patterns and processes revealed by our analyses across different types of temperate forests that vary in their climate and evolutionary history. To test underlying local mechanisms, we simulated spatially explicit 'null communities' that maintain the observed richness and relative abundances of species in each plot (i.e., we removed regional species-pool effects), but randomize tree locations within each plot following spatial point process models that resemble different (null) hypotheses on the presence or absence of dispersal limitation, habitat filtering and interspecific species interactions (Wang et al., 2015; Wiegand & Moloney, 2014). We then compared the simulated patterns with their observed counterparts (Morlon et al., 2008; Shen et al., 2009; Wang et al., 2011; Wiegand & Moloney, 2014). To explore the relative importance of these processes at different ontogenetic stages, we conducted separate analyses for large trees [tree diameter at 1.3 m aboveground (dbh)  $\geq 10$  cm] and small trees (dbh  $< 10$  cm). We asked the following questions. (a) What is the relative importance of species replacement and species nestedness in determining spatial community dissimilarity at different spatial scales? (b) How do dispersal limitation, habitat filtering and interspecific species interactions influence species replacement and nestedness, and do these processes differ among ontogenetic stages? We describe specific hypotheses and predictions for each of these mechanisms below.

## 2 | MATERIALS AND METHODS

### 2.1 | Study sites: Temperate forest-dynamics plots in northern China and northern U.S.A.

Eight large (20–35 ha) temperate forest-dynamics plots were used in the present study (Table 1). Four plots are located in northern China and four in the northern U.S.A. The plots range in latitude from 38.52 to 48.08° N. Total species richness among the plots ranges from 36 to

TABLE 1 Characteristics of the eight Forest Global Earth Observatory (ForestGEO) plots in northern China and northern U.S.A.

Plot	Area (ha)	Latitude	Longitude	Elevation (m)	Mean temperature (°C)	Mean precipitation (mm)	Total species richness	Total number of individuals	Species richness, large trees <sup>a</sup>	Total number of large trees	Species richness, small trees <sup>b</sup>	Total number of small trees
Wabikon, U.S.A. (WAB)	25.2	45.55	-88.79	488–514	4.2	748	36	48,858	23	14,021	33	34,837
Harvard Forest, U.S.A. (HF)	35	42.54	-72.18	340–368	8.8	1,150	55	77,536	34	23,901	53	53,635
Smithsonian Conservation Biology Institute, U.S.A. (SCBI)	25.6	38.89	-78.15	273–338	12.8	1,029	61	29,914	49	8,269	53	21,645
Tyson Research Center, U.S.A. (TRC)	20	38.52	-90.56	172–233	13.6	992	46	37,488	39	6,521	42	30,967
Fenglin, China (FL)	30	48.08	129.12	401–492	-0.5	684	46	94,912	25	11,242	44	83,670
Changbaishan, China (CBS)	25	42.38	128.08	792–810	3.6	700	51	34,926	30	10,329	48	24,597
Baihe, China (BH)	24	42.33	128.01	781–802	3.6	700	63	65,746	34	17,197	60	48,549
Donglingshan, China (DLS)	20	39.96	115.43	1,290–1,509	4.8	650	51	52,682	36	9,558	51	43,124

<sup>a</sup>Diameter at breast height  $\geq 10$  cm.

<sup>b</sup>Diameter at breast height  $< 10$  cm.

63 (Table 1). All free-standing woody stems (excluding lianas) with dbh  $\geq 1$  cm were mapped, tagged, measured and identified to species using standardized ForestGEO protocols (Anderson-Teixeira et al., 2015; Bourg, McShea, Thompson, McGarvey, & Shen, 2013; Condit, 1998).

## 2.2 | Partitioning community dissimilarity into abundance-based species replacement and nestedness

For each forest plot, we were interested in the local-scale ( $< 250$  m) pattern of distance decay of community similarity and its components. Therefore, we combined the analytical framework of decomposing community dissimilarity into nestedness and replacement components (Baselga, 2010, 2017; Legendre, 2014) with the distance-centred framework of spatial point pattern analysis (Shen et al., 2009; Wang et al., 2015; Wiegand & Moloney, 2014; Wiegand et al., 2017). To obtain distance-dependent dissimilarity measures, we resampled the data of the fully mapped plots with the spatial grain of  $20 \text{ m} \times 20 \text{ m}$  subplots. This grain is commonly used in the analysis of ForestGEO plots, and it is also the typical size of patches used in forest gap models (e.g., Fischer et al., 2016). The number of trees and species in these subplots is large enough for meaningful analysis (Supporting Information Table S1).

In a first step of the estimation of distance-dependent dissimilarity measures, we randomly located within a given forest plot 500 pairs of subplots that were distance  $r$  apart. For each subplot  $i$ , we then determined the abundance  $a_{s,i}$  of species  $s$ . Second, we followed Legendre (2014) and Baselga (2017) and calculated the three abundance-based dissimilarity indices  $TD_{ij}$ ,  $Repl_{ij}$  and  $Nes_{ij}$  for the 500 pairs of subplots  $i$  and  $j$  (see Supporting Information Appendix S1 for detail).  $TD_{ij}$  is the total dissimilarity in species abundances between subplot  $i$  and  $j$  as measured by the Ružička index (an abundance-weighted Jaccard index),  $Repl_{ij}$  is the replacement component of  $TD_{ij}$ , and  $Nes_{ij}$  is the nestedness component, with  $TD_{ij} = Repl_{ij} + Nes_{ij}$ . In the third step, we took the mean of  $TD_{ij}$ ,  $Repl_{ij}$  and  $TD_{ij}$  over the 500 pairs of plots that were distance  $r$  apart to obtain our final measures,  $mTD(r)$ ,  $mRepl(r)$  and  $mNes(r)$ . This procedure was repeated for all distances  $r$  of 21–250 m in steps of 1 m. We used the 21–250 m distance range because subplots with  $r \leq 20$  m show substantial spatial overlap, and because for distances  $> 250$  m focal subplots have only a few neighbour subplots at distance  $r$  inside the plot (Wiegand & Moloney, 2014).

## 2.3 | Environmental variables

Two of our five null community models considered the impact of environmental variables on species distribution. We followed an established approach in point process theory and modelled the spatially variable intensity function  $\lambda_i(\mathbf{x})$  at location  $\mathbf{x}$  for each species  $i$  by the log-linear regression model  $\lambda_i(\mathbf{x}) = \exp[\beta_0 + \beta_1 v_1(\mathbf{x}) + \dots + \beta_n v_n(\mathbf{x})]$  with environmental variable  $v_i(\mathbf{x})$  and coefficients  $\beta_i$  that were fitted to the data using maximum likelihood estimation (Waagepetersen & Guan, 2009). For species with  $< 20$  individuals, we used the plot-scale density  $\lambda_i$ , being the number of species divided by the area of the plot.

We followed Wang et al. (2011, 2015) and used six environmental variables (elevation, slope, aspect, terrain convexity, topographic wetness index and altitude above channels) with a spatial resolution of  $5 \text{ m} \times 5 \text{ m}$ . Elevation, slope, aspect and terrain convexity are widely used topographical variables. The other two indices, topographic wetness index (TWI) and vertical distance to the channel network (Chn), are used to compute topographical control on hydrological processes (Kanagaraj, Wiegand, Comita, & Huth, 2011; Punchi-Manage et al., 2013). TWI represents the ratio of the area upslope of each quadrat to the local slope for that quadrat, which can capture important information on wetness. To calculate TWI, we used Tarboton's deterministic infinity method, described by Tarboton (1997) and Sørensen, Zinko, and Seibert (2006), implemented in the open-source software SAGA-GIS (Conrad et al., 2015). The vertical distance from the channel network (i.e., drainage lines of surface rainfall) was also calculated in SAGA-GIS.

## 2.4 | Ecological processes and hypotheses

We generated five types of spatially explicit null communities representing different hypotheses on the relative roles of dispersal limitation, habitat filtering and interspecific species interactions in community assembly. They are based on explicit maps of the locations of the individuals (instead of the number of individuals of species  $s$  in site  $i$ ), and this additional structural realism allows us to devise null models with more direct biological interpretation. All null communities conserved the species richness and relative abundances of species at each plot and were assembled by independent superposition of the distribution patterns of individual species simulated by specific point process models. This corresponds to the assumption of no species interactions (e.g., McGill, 2010; Wiegand et al., 2012). The algorithms of the specific point process models have been described in detail by Wiegand & Moloney (2014) and Wang et al. (2015). Here, we briefly summarize the basic framework of these point process models used to test the five hypotheses below.

### 2.4.1 | The random-placement hypothesis

This hypothesis assumes that all individuals in the study area are randomly and independently distributed. It represents the extreme case of communities without spatial structure that do not, therefore, show distance dependence in spatial community dissimilarity and its components. To implement the random-placement hypothesis, we used for each species  $i$  a homogeneous Poisson process model with the observed intensity  $\lambda_i$  (Illian, Penttinen, Stoyan, & Stoyan, 2008) that assigns each tree a random location within the given study area. Significant deviations from this null model indicate the existence of non-random spatial structures in spatial community dissimilarity, species replacement and nestedness.

### 2.4.2 | The habitat-filtering hypothesis

This hypothesis assumes that the distribution of each species is only driven by local habitat suitability, but all further mechanisms of species patterning are removed. To test the habitat filtering hypothesis, we

used for each species  $i$  an inhomogeneous Poisson process model (Shen et al., 2009), where the habitat suitability at location  $\mathbf{x}$  is represented by the intensity function  $\lambda_i(\mathbf{x})$  (see section 2.3 'Environmental variables' above). If a species did not show significant relationships with environmental variables, we used the constant plot-scale density  $\lambda_i$  instead of  $\lambda_i(\mathbf{x})$ . The inhomogeneous Poisson process produces species patterns where the local density of individuals is proportional to the local habitat suitability given by  $\lambda_i(\mathbf{x})$ , but no additional mechanisms of species aggregation are considered. Significant deviations from this null model indicate that mechanisms and processes beyond habitat filtering are operating. However, departures may also be caused by missing environmental variables or extinction–recolonization dynamics where not all suitable areas are occupied by the species.

#### 2.4.3 | The dispersal-limitation hypothesis

This hypothesis assumes that the community is assembled only by the effects of intraspecific aggregation or inhibition mechanisms of population dynamics (e.g., dispersal limitation or negative conspecific density dependence) without consideration of the influences of habitat filtering or interspecific species interactions. To implement this hypothesis, we used a homogeneous nonparametric annealing algorithm (Tscheschel & Stoyan, 2006; Wiegand, He, & Hubbell, 2013) that is able to create, for each species, null-distribution patterns that closely match the spatial structure of the original pattern as captured by summary functions, such as the pair correlation function, the K-function and the  $k$ th nearest neighbour functions (for detail, see Wiegand et al., 2013). Note that this homogeneous algorithm does not preserve the spatial intensity function  $\lambda_i(\mathbf{x})$  of species  $i$ , but it preserves the observed overall aggregation (that can be co-determined by habitat filtering). Significant deviations from this null model indicate that habitat filtering and/or interspecific species interactions contribute to the observed patterns.

#### 2.4.4 | The combined habitat and dispersal hypothesis

This hypothesis assumes that the community is driven by the joint effects of habitat filtering and dispersal limitation. We created null communities like those generated by the dispersal-limitation hypothesis, but the relocation of individuals of species  $i$  was additionally constrained by the spatial intensity function  $\lambda_i(\mathbf{x})$  used in the habitat filtering hypothesis (Wiegand et al., 2013). Significant deviations from this null model may result from unmeasured environmental factors that are ignored in the log-linear regression models and by interspecific species interactions that are not considered (because the individual species patterns are independently superimposed).

#### 2.4.5 | The independent-placement hypothesis

This hypothesis tests for local interspecific interactions by randomizing species independently of one another, while preserving the overall intraspecific aggregation and the observed larger-scale distribution [i.e., the observed intensity function  $\lambda_i(\mathbf{x})$ ]. Thus, individuals of different species are placed at smaller scales without regard to each other (McGill, 2010). To test this hypothesis, we used the method of the combined habitat and dispersal hypothesis, but a nonparametric kernel estimate

of  $\lambda_i(\mathbf{x})$  with bandwidth  $R$  (Wiegand et al., 2013) replaced the parametric estimate. The nonparametric estimate basically smoothes the observed distribution pattern and therefore faithfully reproduces the observed larger-scale variation in local tree density. Significant deviations from this null model can therefore happen only at distances  $r$  smaller than the bandwidth  $R$ , and mainly as a result of local interspecific species interactions (or imperfect pattern reconstructions or small-scale edaphic factors). We used a bandwidth of  $R = 50$  m, like Wiegand, Gunatilleke, Gunatilleke, and Huth (2007) and Wang et al. (2015) (see Supporting Information Appendix S2).

### 2.5 | Evaluating the fit of the different hypotheses

We calculated the scale-dependent dissimilarity summary functions  $S_i(r)$  [i.e., representing total dissimilarity  $mTD(r)$ , species replacement  $mRepl(r)$  or nestedness  $mNes(r)$ ] for the null communities generated by the five point process models in the same way as for the observed data. To compare the observed summary functions  $S_0(r)$  (indicated by subscript  $i = 0$ ) and that resulting from  $i = 1, \dots, 100$  realizations of the null community models, we first calculated the standardized effect sizes (SES), as follows:

$$SES_i(r) = [S_i(r) - \bar{S}(r)] / \sigma_S(r), \quad (1)$$

where  $\bar{S}(r)$  and  $\sigma_S(r)$  are the mean and the SD of the summary functions  $S_i(r)$  of the 100 null community realizations, respectively. For a given distance  $r$ , the null community model can then be accepted with a 'pointwise' significance level of  $\alpha$  if  $-z_\alpha < SES_0(r) < z_\alpha$ . For  $\alpha = .05$ , we have  $z_\alpha = 1.96$  (Wiegand, Grabarnik, & Stoyan, 2016). That means that we test whether the observed summary function  $S_0(r)$  is located within the 2.5th and 97.5th percentiles of the corresponding null model distributions [i.e., the pointwise simulation envelopes  $S^-(r) = \bar{S}(r) - z_\alpha \sigma_S(r)$  and  $S^+(r) = \bar{S}(r) + z_\alpha \sigma_S(r)$ ; black dashed lines in Figure 1a]. The standardized effects sizes therefore transform the original summary functions in a way that the resulting pointwise simulation envelopes are constants  $-z_\alpha$  and  $z_\alpha$  (Figure 1b) (Wiegand et al., 2016). The standardized effect size is a measure of fit that considers the stochasticity of the null communities. If the stochasticity is large, for example owing to small sample sizes, the observed communities may not be distinguishable from null communities.

To assess the significance of the observed dissimilarity functions over a given distance interval (e.g., 21–250 m), it is important to control for type I error that results from the  $b$  multiple tests conducted at the different distance bins  $r$ . To correct for this effect, we used the simulation-based version of the global envelope test presented by Wiegand et al. (2016) that applies the standard 'maximal absolute difference' (MAD) test to the transformed summary functions  $SES_i(r)$  (Myllymäki, Mrkvicka, Grabarnik, Seijo, & Hahn, 2017). We first estimated the maximal absolute value  $S_i^{\max}$  of  $SES_i(r)$  (over  $r = 21, \dots, 250$ ), where the upper global envelope  $z_\beta$  is the fifth highest value of the  $S_i^{\max}$  (over  $i = 1, \dots, 100$ ), and the lower global envelope is  $-z_\beta$  (red dashed lines in Figure 1b). We found that  $z_\beta$  was c. 3.4. The null hypothesis can be rejected with significance level of  $\alpha = .05$  if the

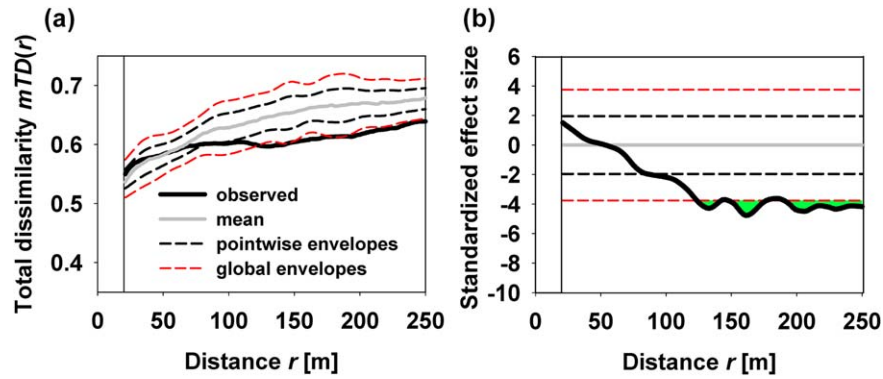


**FIGURE 1** Determining significant departures from the null communities. (a) The observed summary function  $S_0(r)$  (black bold line), the mean  $\bar{S}(r)$  of the summary functions  $S_i(r)$  of the 100 null community realizations (bold grey line), the pointwise simulation envelopes being the 2.5th and 97.5th percentiles of the distribution of the null model simulations  $S_i(r)$  (dashed black line) and the global simulation envelopes for the 21–250 m distance interval (red dashed lines) that correct for multiple testing. (b) Same as (a), but for the summary functions transformed to standardized effect sizes (Equation 1). Note that the resulting simulation envelopes are constants. This allows us to define the index  $Err$  that describes the mean magnitude of departure from the null communities over the 21–250 m distance interval (the green area)

observed summary functions wander at one (or more) distance bins  $r$  outside the global envelopes.

To obtain an index  $Err$  of the overall strength of departure of a given null community model from the observed data over a given distance interval, we estimated the average of the significant component of  $SES(r)$  (i.e., the green area in Figure 1b) over the 21–250 m distance interval:

$$err(r) = \begin{cases} 0 & \text{if } -z_\beta \leq SES(r) \leq z_\beta \\ |SES(r)| - z_\beta & \text{otherwise} \end{cases}$$

$$Err = \frac{1}{b} \sum_{r=r_{\min}}^{r_{\max}} err(r) \quad (2)$$

We have  $Err = 0$  if the null hypothesis is accepted over the interval  $(r_{\min}, \dots, r_{\max})$ , and as a rule of thumb, small departures from the null

hypothesis occur for values of  $Err < 1$  (Wiegand et al., 2016). For the pointwise test (i.e.,  $b = 1$ ),  $Err = 1$  means that the null hypothesis is accepted with a significance level of  $\alpha = .05$  (that results in  $z_\alpha = 1.96$ ), but would be rejected with a significance level of  $\alpha = .003$  (that results in  $z_\alpha = 2.96$ ).

### 3 | RESULTS

#### 3.1 | Observed patterns of spatial community dissimilarity and its components

Spatial community dissimilarity  $mTD(r)$  generally increased with spatial distance  $r$  in all eight temperate forests (Figure 2); only in the Tyson Research Center (TRC) forest did it decrease at larger distances (Figure 2a,e). The three plots [Fenglin (FL), Changbaishan (CBS) and

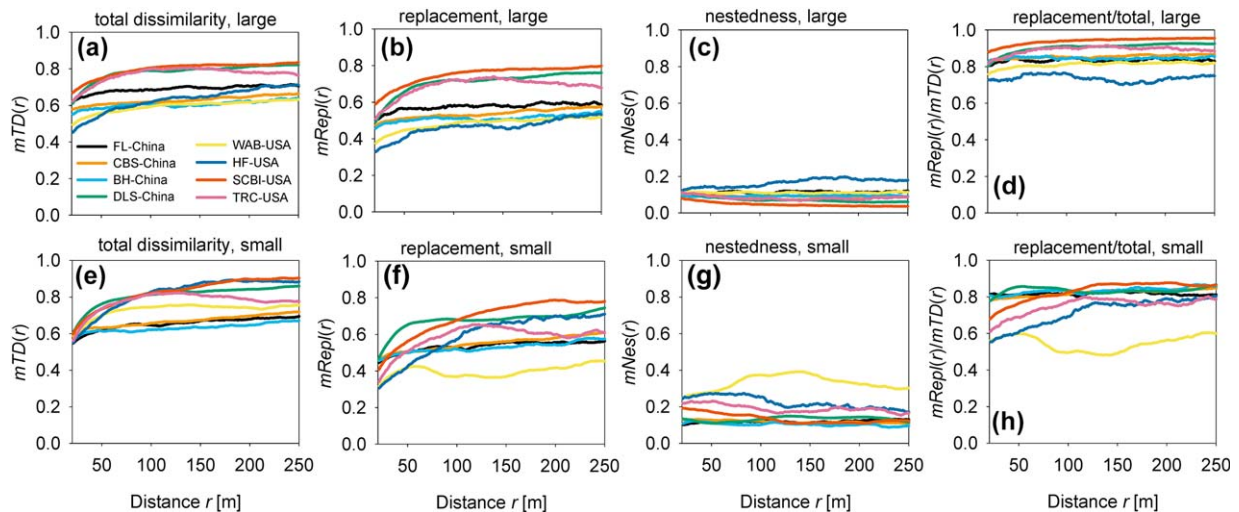


**FIGURE 2** (a–c, e–g) The observed spatial community dissimilarities [ $mTD(r)$ ,  $mRepl(r)$  and  $mNes(r)$ ] in the eight temperate forest plots. Large = individuals with diameter at breast height (dbh)  $\geq 10$  cm; Small = individuals with dbh  $< 10$  cm. Total = total spatial community dissimilarity. (d, h) The proportion of total spatial community dissimilarities attributed to the replacement component.

**TABLE 2** The mean error *Err* (Equation 2) describing the fit of the different null community models for distances  $r = 21\text{--}250$  m for large trees and small trees (in parentheses) in the eight forests

Country	Plots	Random placement	Habitat filtering	Hypothesis		Independent placement
				Dispersal limitation	Habitat and dispersal	
A) Total dissimilarity						
China	FL	7.1 (63.3)	6.8 (30.3)	0.0 (1.3)	0.0 (0.0)	0.0 (0.3)
China	CBS	2.9 (28.9)	0.5 (14.0)	0.0 (0.0)	0.0 (0.4)	0.0 (0.0)
China	BH	12.0 (42.3)	4.4 (20.7)	0.9 (0.5)	0.0 (0.5)	0.1 (0.9)
China	DLS	20.6 (67.6)	8.4 (12.7)	0.0 (0.7)	0.9 (1.5)	0.0 (0.0)
U.S.A.	WAB	8.2 (48.6)	2.7 (9.0)	0.3 (0.5)	0.0 (0.0)	0.0 (0.0)
U.S.A.	HF	19.0 (71.7)	7.0 (8.1)	0.0 (1.4)	0.5 (0.3)	0.0 (0.0)
U.S.A.	SCBI	5.8 (35.5)	2.1 (6.9)	0.0 (0.1)	0.0 (0.4)	0.0 (0.0)
U.S.A.	TRC	11.3 (63.1)	2.0 (4.5)	0.0 (2.5)	0.2 (1.8)	0.0 (0.0)
B) Replacement component						
China	FL	4.4 (40.4)	4.2 (37.2)	0.0 (0.6)	0.3 (0.2)	0.5 (0.0)
China	CBS	3.4 (19.7)	1.7 (15.2)	0.3 (0.4)	1.0 (0.3)	0.0 (0.0)
China	BH	10.4 (26.0)	5.9 (18.3)	0.4 (0.0)	3.1 (4.7)	0.9 (0.0)
China	DLS	20.3 (52.5)	8.5 (14.1)	1.0 (0.4)	1.3 (1.7)	0.0 (0.0)
U.S.A.	WAB	4.5 (10.4)	4.4 (14.8)	0.0 (1.4)	0.7 (3.4)	0.3 (0.0)
U.S.A.	HF	9.2 (34.3)	1.3 (13.5)	0.0 (0.3)	0.2 (3.0)	0.0 (0.0)
U.S.A.	SCBI	5.4 (27.3)	3.0 (4.3)	0.3 (0.0)	0.3 (0.5)	0.4 (0.0)
U.S.A.	TRC	9.9 (42.7)	2.8 (7.2)	0.7 (1.3)	0.2 (3.4)	0.0 (0.0)
C) Nestedness component						
China	FL	0.0 (9.3)	0.0 (3.1)	0.0 (0.0)	0.7 (0.0)	0.1 (0.0)
China	CBS	0.4 (2.0)	1.0 (1.5)	0.6 (0.1)	1.6 (0.0)	0.3 (0.0)
China	BH	0.1 (3.8)	0.8 (1.0)	0.4 (0.3)	3.7 (4.2)	0.4 (0.0)
China	DLS	1.7 (11.7)	1.5 (1.9)	0.8 (0.0)	1.2 (1.4)	0.6 (0.0)
U.S.A.	WAB	0.0 (34.2)	1.4 (0.0)	0.9 (0.8)	1.5 (0.8)	0.8 (0.0)
U.S.A.	HF	5.2 (25.5)	6.3 (2.1)	0.7 (2.9)	4.1 (3.5)	0.0 (0.0)
U.S.A.	SCBI	1.5 (4.8)	1.3 (0.0)	0.7 (0.1)	1.3 (0.5)	0.4 (0.0)
U.S.A.	TRC	0.9 (13.6)	0.6 (1.2)	0.8 (0.7)	0.7 (3.2)	0.2 (0.0)

Note. For  $Err = 0$ , the null hypothesis is accepted with significance level of .05 over the entire distance interval; weak departures from the null hypothesis occur for values of  $Err < 1$ .

Baihe (BH)] in northern China showed only a weak increase of dissimilarity with distance, whereas the Donglingshan (DLS) plot in northern China and the Harvard Forest (HF) plot in the northern U.S.A. showed strong increases (Figure 2a,e). In general, the communities of small trees showed stronger increases in dissimilarity with distance than the communities of large trees.

In all eight forests, spatial community dissimilarity was primarily related to species replacement among local assemblages distance  $r$  apart (Figure 2d,h). For large trees, we found that between 70 and 96% of the dissimilarity (at distances  $> 20$  m) could be attributed to the species replacement component (Figure 2d). The largest contribution of species replacement occurred at the Smithsonian Conservation Biology Institute (SCBI) plot (c. 94%; red line in Figure 2d) and the lowest for the HF plot (c. 74%; blue line in Figure 2d). We observed similar patterns for small trees at all four plots in northern China (between 78 and 87%); however, for small trees at the plots in northern U.S.A. the nestedness component became more important at scales between 20 and 100 m (Figure 2h), and at the Wabikon (WAB) forest it even accounted for half of the dissimilarity. The absolute nestedness values for large trees and small trees in northern China showed relatively little response to spatial scale (Figure 2c,g), but nestedness of small trees decreased at intermediate scales at the plots in northern U.S.A. (Figure 2g).

### 3.2 | Relative importance of dispersal limitation, habitat filtering and interspecific interactions

#### 3.2.1 | The replacement component

The random placement hypothesis, which represents communities without any spatial structure, yielded the poorest fit to the observed replacement components for both large and small trees (Table 2B; Supporting Information Figure S2). The index *Err* of departures from the null community ranged for large trees between 3.4 and 20.3 and for small trees between 10.4 and 52.5 (Table 2B). The mean strength of departures *Err* from random placement were much larger for small trees, especially for the FL, DLS, HF and TRC plots. Interestingly, the index *Err* was correlated with the elevation range of the plots shown in Table 1 (correlation coefficients were 0.78 for large trees and 0.77 for small trees). The habitat filtering hypothesis, which accounted for the effects of topographic variables, improved the fit in most cases, but still produced highly significant departures, with *Err* ranging between 1.3 and 8.5 for large trees and between 4.3 and 37.2 for small trees (Table 2B).

In most cases, the dispersal-limitation hypothesis fitted the observed replacement component (i.e.,  $Err = 0$ ) or produced only small departures (i.e.,  $Err \leq 1$ ; Table 2B). The more complex combined habitat and dispersal limitation hypothesis produced similar good fits for large

trees (except the BH plot), but for smaller trees in the BH, WAB, HF and TRC plots larger departures (with  $Err > 2$ ). The independent-placement hypotheses fitted the observed replacement component in all eight plots (smaller departures for large trees in BH and SCBI, otherwise  $Err = 0$ ) for both the large and small tree communities (Table 2B).

### 3.2.2 | The nestedness component

The nestedness component of community dissimilarity was driven by different mechanisms than the replacement component. For large trees, we found that random placement produced surprisingly good approximations of the nestedness component (with  $Err < 1.7$ ), except at the HF forest, with  $Err = 5.2$ , which showed the largest nestedness component for large trees among all eight forests (Table 2C). Habitat filtering produced good fits, similar to random placement (Supporting Information Figure S3). The dispersal-limitation hypothesis also produced only weak departures (i.e.,  $Err \leq 1$ ) for the HF forest.

For small trees, in contrast, random placement did not fit the observed nestedness components and produced large departures for some forests, especially for the WAB ( $Err = 34.2$ ) and HF ( $Err = 25.5$ ) forests. Habitat filtering improved the fit substantially in all cases, including the WAB and SCBI forests, yielding otherwise only weak departures (Table 2C). Dispersal limitation produced only weak departures, except for the HF plot (Table 2C). The independent-placement hypothesis fitted the data well in all cases.

### 3.2.3 | Total dissimilarity

In general, the null model analyses yielded similar results for total dissimilarity and the replacement component (cf. Table 2A,B; Supporting Information Figure S1). Here, the dispersal-limitation hypothesis and the combined habitat and dispersal hypothesis produced similar fits, with  $Err < 1$ , in most cases. Notably, the combined habitat and dispersal hypothesis produced better fits for total dissimilarity than its replacement component (Table 2A).

## 4 | DISCUSSION

In this study, we evaluated the relative importance of two complementary processes (species replacement and nestedness) underlying tree community dissimilarity measures (Baselga, 2010; Legendre, 2014; Podani & Schmera, 2011) in eight fully mapped ForestGEO plots in the U.S.A. and China (Anderson-Teixeira et al., 2015). We used spatial point pattern analysis and spatially explicit null models (Wang et al., 2015; Wiegand & Moloney, 2014; Wiegand et al., 2017) to analyse mechanisms underlying observed patterns in the two dissimilarity components. Our study yielded three key findings. First, total spatial community dissimilarity was primarily driven by species replacement among local assemblages. The species-replacement components and total dissimilarity generally increased with spatial distances, whereas the species-nestedness component showed little response to spatial scale. Second, the dispersal-limitation hypothesis provided the best explanation for species replacement and total dissimilarity, whereas the

association of species to topographic variables (i.e., the habitat-filtering hypothesis) provided mostly poor fits. However, nestedness of large trees was also well fitted by the random placement and habitat filtering hypotheses, and for small trees nestedness was also well fitted by the habitat filtering hypothesis. Third, we found that the nestedness components of the plots in the northern U.S.A. varied in general more than that in northern China. This was especially true for small trees, where nestedness values of the northern U.S.A. plots were substantially larger than those in northern China. Overall, our results support the hypothesis that the two components of spatial community dissimilarity are driven by different mechanisms of community assembly.

### 4.1 | The relative importance of the replacement and nestedness components

In all eight forest plots, we found that patterns of community dissimilarity primarily reflected species replacement among local communities. Overall, we obtained similar results from forest plots in northern China and northern U.S.A. However, the contributions of the nestedness components to total dissimilarities were higher in northern U.S.A., especially at distances  $< 100$  m. The generally low contribution of nestedness to overall dissimilarity of local species assemblages can be explained by the relatively small local variation in species richness among local communities (i.e.,  $20\text{ m} \times 20\text{ m}$  subplots). We found that the high nestedness component of small trees at the WAB and HF forests coincided with a high local variation in species richness (coefficient of variation = 0.54 and 0.62) and number of individuals (coefficient of variation = 0.95 and 1.21), a pattern inevitably leading to 'diversity hotspots' (Supporting Information Table S1). This observation parallels the high degree of nestedness found within island archipelagos (Lomolino, 1996; Si, Baselga, Ding, & Machado, 2015), where selective immigration and extinction lead to ordered patterns of species assemblages. In particular, depauperate islands tend to be occupied by predictable subsets of species occurring on species-rich islands. In contrast, smaller variation in local richness, as observed for large trees and small trees at the plots in northern China, leaves little room for typical nestedness configurations with strong spatial richness gradients or 'hotspots' of local species richness (or tree abundance).

The relatively large nestedness component for small trees in the northern U.S.A. forests is probably related to their overall lower species richness that scales down to the low mean species richness of small trees at the subplot scale (ranging between 4.9 and 6.9 in northern U.S.A. and between 7.6 and 13.7 in northern China; Supporting Information Table S1). Interestingly, all plots showed for small trees a similar  $SD$  in local species richness (c. 2.7; Supporting Information Table S1), which then results in higher local variation in richness of the North American plots (Supporting Information Table S1). For example, the WAB and HF forest plots, with the high nestedness values for small trees, both show patchy local hotspots of high density (and richness) of small trees. The generation of local hotspots of species richness at these two plots was probably enhanced by localized logging during the 1900s at WAB and following a hurricane of 1938 at HF.

## 4.2 | Ecological mechanisms underlying replacement and nestedness

Habitat filtering and dispersal limitation have been regarded as two major mechanisms of community assembly, but their relative roles across forests remains elusive. Our results showed consistently for all forests that the dispersal-limitation hypothesis (i.e., maintaining the observed intraspecific aggregation) contributed more to the average total compositional dissimilarity between local communities than habitat filtering. This result is consistent with previous studies in tropical (Morlon et al., 2008) and temperate forests (Wang et al., 2011). Moreover, this general finding challenges the idea that dispersal assembly may be relatively more important than niche assembly in high-diversity (e.g., tropical) compared with low-diversity (e.g., temperate) forest communities (Hubbell, 2001; Myers et al., 2013); our results suggest that it is important universally.

Our study advances previous work on the processes governing distance decay of similarity at local scales (e.g., Morlon et al., 2008; Wang et al., 2011, 2015) by separate analysis of the species replacement and nestedness components of spatial community dissimilarity. We found that the species replacement component was able to discriminate clearly among competing hypotheses. Our analysis led to acceptance of the dispersal limitation hypotheses as the simplest hypotheses that fitted the observations reasonably well, clearly rejecting the random placement and habitat filtering hypotheses. However, the nestedness component was influenced by different processes. The random-placement hypothesis explained the low species-nestedness component for large trees well (except for the HF forest, which showed the largest nestedness component for large trees), suggesting that spatial distributions of large trees may be strongly influenced by stochastic community assembly resulting from ecological drift (Hubbell, 2001). In contrast, the habitat-filtering hypothesis provided a better explanation for the larger species-nestedness components of small trees (especially at the WAB forest), suggesting a stronger influence of deterministic community assembly at earlier life stages or for understorey species relative to canopy species.

The inability of the habitat-filtering models to explain observed spatial community dissimilarities can be explained partly by effects of from extinction–recolonization dynamics (where not all species occupy all suitable areas) or from the omission of some important environmental variables. For instance, soil nutrients such as nitrogen, phosphorus and aluminum have been shown to influence local spatial distributions of species in tropical (e.g., Condit, Engelbrecht, Pino, Pérez, & Turner, 2013; John et al., 2007) and temperate (LaManna, Walton, Turner, Myers, & Rejmanek, 2016; Spasojevic, Turner, Myers, & Jones, 2016) forests. Also, factors such as land-use history (e.g., grazing, hunting and logging) may have affected the spatial pattern of species, especially at the WAB and SCBI plots, where historical logging is known to have occurred. Given a lack of more detailed environmental data, we leave this as an issue for forthcoming studies.

In addition, we found that patterns of species nestedness and replacement were influenced by variation in local species richness and densities of individuals at the 20 m × 20 m subplot scale. At the local

scales analysed here, we find that the replacement component accounts for spatial community dissimilarity caused by 'homogeneous' species clustering as described by the dispersal limitation hypothesis (i.e., species clusters of different species are independent and can appear everywhere in the plot with the same probability). This is also the spatial pattern expected from neutral theory (Hubbell, 2001). In contrast, the spatial nestedness component of spatial dissimilarity can only become more important if the community shows high heterogeneity in local species richness and/or local individual numbers. Otherwise, in more homogeneous communities, nestedness remains small and arises from stochasticity as captured by random placement.

## 4.3 | Effects of interspecific species interactions

Surprisingly, our results suggest that small-scale species interactions have a relatively weak influence on overall spatial patterns of community dissimilarity in the temperate forests analysed. The independent-placement hypothesis that distributes individuals of a species locally irrespective of individuals of other species (McGill, 2010; Wiegand et al., 2012) generated excellent approximations of spatial community dissimilarity, species replacement and nestedness in all forests at distances of 21–250 m (Table 2). This result is inconsistent with previous studies that have provided evidence for the importance of pairwise interspecific species interactions, especially for tree species in temperate forests (e.g., Canham et al., 2006; Wang et al., 2010). For instance, Wang et al. (2010) found that c. 30% of all pairs of large tree species showed evidence of interspecific interactions at the CBS plot. Possible explanations for this finding are that the effects of significant negative pairwise interspecific interactions on community level patterns might be 'diluted' by the non-significant interactions (e.g., the 60% found by Wang et al., 2010) or by stochasticity (Wang et al., 2016), or the effect of positive and negative pairwise interspecific interactions on community level patterns might cancel one another. As a consequence, significant pairwise interactions might leave no strong signal in community-level patterns such as the species–area relationship and spatial community dissimilarity (Wang et al., 2011).

An alternative but complementary explanation for our reported patterns is that the detectable small-scale interactions in some of the species pairs translated only into subtle small-scale patterns that are not detectable with the relatively coarse 20 m spatial resolution used here. For example, Wang et al. (2015) detected at scales < 15 m subtle effects of interspecific interactions in patterns of phylogenetic and functional beta diversity (their fig. D6 in appendix D) quantified by high-resolution point pattern summary functions not based on subplot counting. Moreover, weak interspecific interactions could result from a relatively stronger influence of intraspecific interactions, such as intraspecific competition for limiting resources or negative density dependence caused by specialized natural enemies (LaManna et al., 2016).

## 4.4 | Conclusions

Analyzing patterns of spatial community dissimilarity, species replacement and species nestedness have substantially advanced our

understanding of the processes controlling macro-scale biodiversity patterns, but the ways in which different community assembly processes create these patterns at local scales remain largely unexplored. Across eight temperate forests in northern China and northern U.S.A., we show that spatial community dissimilarity is primarily explained by species replacement among local assemblages. Moreover, we show that different assembly processes influence the species replacement and species nestedness components of community dissimilarity. Species replacement of both large and small trees was primarily explained by dispersal limitation in all forests, whereas small nestedness was primarily associated with stochastic processes (random spatial distributions of large trees), and larger nestedness (of small trees) was primarily associated with larger heterogeneous variability in local species richness. In contrast, interspecific species interactions appeared to have no detectable influence on spatial community dissimilarity and its replacement and nestedness components across all forests. Collectively, these results indicate that the species replacement and nestedness components of community patterns provide key insights into the relative importance of different ecological processes underlying community assembly and local biodiversity patterns; these insights could easily be overlooked in studies that focus solely on patterns of community dissimilarity. Thus, the novel use of replacement and nestedness measures in point pattern analysis of large, fully mapped forest dynamics plots is a promising approach to assess local-scale biodiversity patterns and to explore their causes.

## ACKNOWLEDGMENTS

This work was supported by National Natural Science Foundation of China (31722010), the Strategic Priority Research Program of the Chinese Academy of Sciences (XDPB0203), National Key Research and Development Program of China (2016YFC0500300) and National Natural Science Foundation of China (31770666, 31570630). Funding for the SCBI plot was provided by the Smithsonian Global Earth Observatory initiative, the Smithsonian Institution, National Zoological Park and the HSBC Climate Partnership. Funding for the Tyson Research Plot was provided by the International Center for Advanced Renewable Energy and Sustainability (I-CARES) at Washington University in St Louis, the National Science Foundation (DEB 1557094 to J.A.M. and M.J.S.) and the Tyson Research Center. Research at the Wabikon Forest Dynamics Plot was supported by The 1923 Fund, the Smithsonian Institution, and the Cofrin Center for Biodiversity at the University of Wisconsin-Green Bay. T.W. was supported by the European Research Council (ERC) advanced grant 233066.

## DATA ACCESSIBILITY

Data on these temperate forest plots are available at <http://www.for-estgeo.si.edu/> and accessible by contacting the principal investigator of each plot.

## AUTHOR CONTRIBUTIONS

X.W. and T.W. designed the study; X.W., T.W. and J.A.M. wrote the manuscript; X.W. performed data analyses; K.J.A.-T., N.A.B., Z.H.,

R.H., G.J., D.A.O., M.J.S., S.W., A.W. and J.A.M. provided data and commented on the manuscript.

## ORCID

Xugao Wang  <http://orcid.org/0000-0003-1207-8852>

Thorsten Wiegand  <http://orcid.org/0000-0002-3721-2248>

Guangze Jin  <http://orcid.org/0000-0002-9852-0965>

## REFERENCES

- Anderson, M. J., Crist, T. O., Chase, J. M., Vellend, M., Inouye, B. D., Freestone, A. L., ... Swenson, N. G. (2011). Navigating the multiple meanings of  $\beta$  diversity: A roadmap for the practicing ecologist. *Ecology Letters*, 14, 19–28.
- Anderson-Teixeira, K. J., Davies, S. J., Bennett, A. C., Gonzalez-Akre, E. B., Muller-Landau, H. C., Joseph Wright, S., ... Zimmerman, J. (2015). CTFS-ForestGEO: A worldwide network monitoring forests in an era of global change. *Global Change Biology*, 21, 528–549.
- Baselga, A. (2010). Partitioning the turnover and nestedness components of beta diversity. *Global Ecology and Biogeography*, 19, 134–143.
- Baselga, A. (2017). Partitioning abundance-based multiple-site dissimilarity into components: Balance variation in abundance and abundance gradients. *Methods in Ecology and Evolution*, 8, 799–808.
- Baselga, A., & Leprieux, F. (2015). Comparing methods to separate components of beta diversity. *Methods in Ecology and Evolution*, 6, 1069–1079.
- Bourg, N. A., McShea, W. J., Thompson, J. R., McGarvey, J. C., & Shen, X. (2013). Initial census, woody seedling, seed rain, and stand structure data for the SCBI SIGEO large forest dynamics plot. *Ecology*, 94, 2111–2112.
- Canham, C. D., Papaik, M. J., Uriarte, M., McWilliams, W. H., Jenkins, J. C., & Twery, M. J. (2006). Neighborhood analyses of canopy tree competition along environmental gradients in New England forests. *Ecological Applications*, 16, 540–554.
- Catano, C. P., Dickson, T. L., Myers, J. A., & Rejmanek, M. (2017). Dispersal and neutral sampling mediate contingent effects of disturbance on plant beta-diversity: A meta-analysis. *Ecology Letters*, 20, 347–356.
- Chase, J. M. (2007). Drought mediates the importance of stochastic community assembly. *Proceedings of the National Academy of Sciences USA*, 104, 17430–17434.
- Chase, J. M., & Myers, J. A. (2011). Disentangling the importance of ecological niches from stochastic processes across scales. *Philosophical Transactions of the Royal Society B: Biological Sciences*, 366, 2351–2363.
- Condit, R. (1998). *Tropical forest census plots: Methods and results from Barro Colorado Island, Panama and a comparison with other plots*. Berlin, Heidelberg: Springer-Verlag.
- Condit, R., Engelbrecht, B. M. J., Pino, D., Pérez, R., & Turner, B. L. (2013). Species distributions in response to individual soil nutrients and seasonal drought across a community of tropical trees. *Proceedings of the National Academy of Sciences USA*, 110, 5064–5068.
- Condit, R., Pitman, N., Leigh, E. G., Chave, J., Terborgh, J., Foster, R. B., ... Hubbell, S. P. (2002). Beta-diversity in tropical forest trees. *Science*, 295, 666–669.
- Conrad, O., Bechtel, B., Bock, M., Dietrich, H., Fischer, E., Gerlitz, L., ... Böhner, J. (2015). System for automated geoscientific analyses (SAGA) v. 2.1.4. *Geoscientific Model Development*, 8, 1991–2007.

- Dobrovolski, R., Melo, A. S., Cassemiro, F. A. S., & Diniz-Filho, J. A. F. (2012). Climatic history and dispersal ability explain the relative importance of turnover and nestedness components of beta diversity. *Global Ecology and Biogeography*, 21, 191–197.
- Fischer, R., Bohn, F., Dantas de Paula, M., Dislich, C., Groeneveld, J., Gutiérrez, A. G., ... Huth, A. (2016). Lessons learned from applying a forest gap model to understand ecosystem and carbon dynamics of complex tropical forests. *Ecological Modelling*, 326, 124–133.
- Greve, M., Gremmen, N. J. M., Gaston, K. J., & Chown, S. L. (2005). Nestedness of Southern Ocean island biotas: Ecological perspectives on a biogeographical conundrum. *Journal of Biogeography*, 32, 155–168.
- Hubbell, S. P. (2001). *The unified neutral theory of biodiversity and biogeography*. Princeton, NJ: Princeton University Press.
- Illian, J., Penttinen, A., Stoyan, H., & Stoyan, D. (2008). *Statistical analysis and modelling of spatial point patterns*. New York: Wiley.
- John, R., Dalling, J. W., Harms, K. E., Yavitt, J. B., Stallard, R. F., Mirabello, M., ... Foster, R. B. (2007). Soil nutrients influence spatial distributions of tropical tree species. *Proceedings of the National Academy of Sciences USA*, 104, 864–869.
- Kanagaraj, R., Wiegand, T., Comita, L. S., & Huth, A. (2011). Tropical tree species assemblages in topographical habitats change in time and with life stage. *Journal of Ecology*, 99, 1441–1452.
- Kneitel, J. M., & Miller, T. E. (2003). Dispersal rates affect species composition in metacommunities of *Sarracenia purpurea* inquilines. *The American Naturalist*, 162, 165–171.
- Kraft, N. J. B., Adler, P. B., Godoy, O., James, E. C., Fuller, S., Levine, J. M., & Fox, J. (2015). Community assembly, coexistence, and the environmental filtering metaphor. *Functional Ecology*, 29, 592–599.
- LaManna, J. A., Walton, M. L., Turner, B. L., Myers, J. A., & Rejmanek, M. (2016). Negative density dependence is stronger in resource-rich environments and diversifies communities when stronger for common but not rare species. *Ecology Letters*, 19, 657–667.
- Legendre, P. (2014). Interpreting the replacement and richness difference components of beta diversity. *Global Ecology and Biogeography*, 23, 1324–1334.
- Lomolino, M. (1996). Investigating causality of nestedness of insular communities: Selective immigrations or extinctions? *Journal of Biogeography*, 23, 699–703.
- McGill, B. J. (2010). Matters of scale. *Science*, 328, 575–576.
- Morlon, H., Chuyong, G., Condit, R., Hubbell, S., Kenfack, D., Thomas, D., ... Green, J. L. (2008). A general framework for the distance-decay of similarity in ecological communities. *Ecology Letters*, 11, 904–917.
- Mouquet, N., & Loreau, M. (2003). Community patterns in source-sink metacommunities. *The American Naturalist*, 162, 544–557.
- Myers, J. A., & LaManna, J. A. (2016). The promise and pitfalls of beta diversity in ecology and conservation. *Journal of Vegetation Science*, 27, 1081–1083.
- Myers, J. A., Chase, J. M., Jiménez, I., Jørgensen, P. M., Araujo-Murakami, A., Paniagua-Zambrana, N., & Seidel, R. (2013). Beta-diversity in temperate and tropical forests reflects dissimilar mechanisms of community assembly. *Ecology Letters*, 16, 151–157.
- Myllymäki, M., Mrkvicka, T., Grabarnik, P., Seijo, H., & Hahn, U. (2017). Global envelope tests for spatial processes. *Journal of the Royal Statistical Society Series B*, 79, 381–404.
- Nekola, J. C., & White, P. S. (1999). The distance decay of similarity in biogeography and ecology. *Journal of Biogeography*, 26, 867–878.
- Podani, J., & Schmera, D. (2011). A new conceptual and methodological framework for exploring and explaining pattern in presence-absence data. *Oikos*, 120, 1625–1638.
- Punchi-Manage, R., Getzin, S., Wiegand, T., Kanagaraj, R., Savitri Gunatilleke, C. V., Nimal Gunatilleke, I. A. U., ... Huth, A. (2013). Effects of topography on structuring local species assemblages in a Sri Lankan mixed dipterocarp forest. *Journal of Ecology*, 101, 149–160.
- Qian, H., & Ricklefs, R. E. (2012). Disentangling the effects of geographic distance and environmental dissimilarity on global patterns of species turnover. *Global Ecology and Biogeography*, 21, 341–351.
- Shen, G., Yu, M., Hu, X., Mi, X., Ren, H., Sun, I., & Ma, K. (2009). Species-area relationships explained by the joint effects of dispersal limitation and habitat heterogeneity. *Ecology*, 90, 3033–3041.
- Si, X., Baselga, A., Ding, P., & Machado, R. B. (2015). Revealing beta-diversity patterns of breeding bird and lizard communities on uninhabited land-bridge islands by separating the turnover and nestedness components. *PLoS One*, 10, e0127692.
- Soininen, J., McDonald, R., & Hillebrand, H. (2007). The distance decay of similarity in ecological communities. *Ecography*, 30, 3–12.
- Sørensen, R., Zinko, U., & Seibert, J. (2006). On the calculation of the topographic wetness index: Evaluation of different methods based on field observations. *Hydrology and Earth System Sciences*, 10, 101–112.
- Spasojevic, M. J., Turner, B. L., Myers, J. A., & Jones, R. (2016). When does intraspecific trait variation contribute to functional beta-diversity? *Journal of Ecology*, 104, 487–496.
- Svenning, J., Fløjgaard, C., & Baselga, A. (2011). Climate, history and neutrality as drivers of mammal beta diversity in Europe: Insights from multiscale deconstruction. *Journal of Animal Ecology*, 80, 393–402.
- Tarboton, D. G. (1997). A new method for determination of flow directions and upslope areas in grid digital elevation models. *Water Resource Research*, 33, 309–319.
- Tscheschel, A., & Stoyan, D. (2006). Statistical reconstruction of random point patterns. *Computational Statistics and Data Analysis*, 51, 859–871.
- Tuomisto, H., Ruokolainen, K., & Yli-Halla, M. (2003). Dispersal, environment, and floristic variation of western Amazonian forests. *Science*, 299, 241–244.
- Waagepetersen, R., & Guan, Y. (2009). Two-step estimation for inhomogeneous spatial point processes. *Journal of the Royal Statistical Society B*, 71, 685–702.
- Wang, X., Wiegand, T., Hao, Z., Li, B., Ye, J., & Lin, F. (2010). Species associations in an old-growth temperate forest in north-eastern China. *Journal of Ecology*, 98, 674–686.
- Wang, X., Wiegand, T., Kraft, N. J. B., Swenson, N. G., Davies, S. J., Hao, Z., ... Wolf, A. (2016). Stochastic dilution effects weaken deterministic effects of niche-based processes in species rich forests. *Ecology*, 97, 347–360.
- Wang, X., Wiegand, T., Swenson, N. G., Wolf, A. T., Howe, R. W., Hao, Z., ... Yuan, Z. (2015). Mechanisms underlying local functional and phylogenetic beta diversity in two temperate forests. *Ecology*, 96, 1062–1073.
- Wang, X., Wiegand, T., Wolf, A., Howe, R., Davies, S. J., & Hao, Z. (2011). Spatial patterns of tree species richness in two temperate forests. *Journal of Ecology*, 99, 1382–1393.
- Whittaker, R. H. (1960). Vegetation of the Siskiyou mountains, Oregon and California. *Ecological Monographs*, 30, 279–338.
- Wiegand, T., & Moloney, K. A. (2014). *Handbook of spatial point pattern analysis in ecology*. Boca Raton, FL: Chapman and Hall/CRC Press.
- Wiegand, T., Grabarnik, P., & Stoyan, D. (2016). Envelope tests for spatial point patterns with and without simulation. *Ecosphere*, 7, e01365.
- Wiegand, T., Gunatilleke, C. V. S., Gunatilleke, I. A. U. N., & Huth, A. (2007). How individual species structure diversity in tropical forests. *Proceedings of the National Academy of Sciences USA*, 104, 19029–19033.

- Wiegand, T., He, F., & Hubbell, S. P. (2013). A systematic comparison of summary characteristics for quantifying point patterns in ecology. *Ecography*, 36, 92–103.
- Wiegand, T., Huth, A., Getzin, S., Wang, X., Hao, Z., Gunatilleke, C. V. S., & Gunatilleke, I. A. U. N. (2012). Testing the independent species' arrangement assertion made by theories of stochastic geometry of biodiversity. *Proceedings of the Royal Society B: Biological Sciences*, 279, 3312–3320.
- Wiegand, T., Uriarte, M., Kraft, N. J. B., Shen, G., Wang, X., & He, F. (2017). Spatially explicit metrics of species diversity, functional diversity, and phylogenetic diversity: Insights into plant community assembly processes. *Annual Review of Ecology, Evolution, and Systematics*, 48, 329–351.

## BIOSKETCH

XUGAO WANG is a professor of forest ecology at Shenyang Institute of Applied Ecology, Chinese Academy of Sciences. His current research

focuses on spatial patterns, dynamics and underlying mechanisms of plant communities in forests.

## SUPPORTING INFORMATION

Additional Supporting Information may be found online in the supporting information tab for this article.

**How to cite this article:** Wang X, Wiegand T, Anderson-Teixeira KJ, et al. Ecological drivers of spatial community dissimilarity, species replacement and species nestedness across temperate forests. *Global Ecol Biogeogr.* 2018;27:581–592. <https://doi.org/10.1111/geb.12719>